Coherence-based beamforming improves the diagnostic certainty of breast ultrasound exams

Alycen Wiacek*, Eniola Oluyemi†, Kelly Myers†, Lisa Mullen† and Muyinatu A. Lediju Bell*‡§
*Department of Electrical and Computer Engineering, Johns Hopkins University, Baltimore, MD
†Department of Radiology and Radiological Science, Johns Hopkins Medicine, Baltimore, MD
‡Department of Biomedical Engineering, Johns Hopkins University, Baltimore, MD
§Department of Computer Science, Johns Hopkins University, Baltimore, MD

***Abstract*—Breast ultrasound is often used as a diagnostic tool to diagnose breast cancer, however the high false positive rate limits its use in screening. Coherence-based beamforming has been shown improve the distinction between solid and fluid breast masses, therefore the objective of this work is to both qualitatively and quantitatively investigate the clinical impact of coherence-based beamforming. Five board-certified breast radiologists were asked to read ultrasound images of twenty-six masses and select the content (i.e., solid, fluid, mixed, or uncertain) and the clinical diagnosis (i.e., BI-RADS 2, 3, 4 or 5). The responses were compared with and without the inclusion of coherence-based beamforming to qualitatively assess the impact of coherence-based beamforming. In addition, coherence-based metrics including lag-one coherence (LOC) and coherence length (CL) were used to quantitatively distinguish solid from fluid-filled masses. When including coherence-based beamforming, the mean reader sensitivity for detection of fluid-filled masses was improved from 57% with B-mode alone to 86% with the addition of coherence-based images. Using LOC as a quantitative metric, with an optimal threshold of 0.3, the sensitivity for detection of fluid-filled masses was further improved to 100% with a specificity of 94%. These results are promising for the inclusion of coherence-based features in the breast clinic in order to improve diagnostic certainty, particularly when distinguishing between solid and fluid-filled breast masses.**

I. Introduction

Ultrasound imaging is often used for the diagnosis of breast cancer because it is painless, radiation-free, and highly portable, however the high false positive rate of breast ultrasound limits its use as a screening tool. Specifically, standard brightness-mode (B-mode) images display amplitude information, which is highly susceptible to the presence of acoustic clutter. Acoustic clutter can arise from multipath acoustic interactions between layers of tissue [1], which confounds masses of interest, and can result in these fluid-filled masses being unnecessarily recommended for biopsy or follow-up procedures.

One method to remove acoustic clutter is through advanced beamforming techniques such as minimum variance [2], multi-covariate imaging of sub-resolution targets (MIST) [3], and short-lag spatial coherence (SLSC) [4]. Our previous work demonstrated that SLSC beamforming and a more recent improvement named Robust SLSC (R-SLSC) beamforming [5] successfully removed acoustic clutter and improved the distinction between solid and fluid breast masses [6]. We additionally investigated the clinical impact of these results in a task-based user study with five board-certified radiologist readers, demonstrating that coherence-based beamforming provides added value in the diagnostic pipeline [7]. The work presented in this paper builds on our previous reader study and analyzes the coherence-based features of each breast mass relative to reader performance, with an overall objective to provide both a qualitative and quantitative investigation of the potential clinical impact of coherence-based beamforming.

II. Methods

A. Data Acquisition

Twenty-five patients with twenty-six breast masses scheduled for biopsy were enrolled in our ongoing study after informed consent and approval from the Johns Hopkins Institutional Review Board. Patients were scanned using an Alpinion ECUBE12R research ultrasound scanner connected to either an Alpinion L8-17 or an Alpinion L3-8 linear ultrasound transducer. Raw radiofrequency data were saved and processed offline to generate matched B-mode and coherence-based images for each mass. In addition, matched clinical screenshots of each mass were saved for comparison. Coherence-based images were created using R-SLSC beamforming [5], which directly displays the denoised spatial coherence of backscattered ultrasound pressure waves.

B. Reader Study

Matched images (i.e., clinical screenshot, delay-and-sum beamformed B-mode image, and corresponding R-SLSC image created from the same channel data) of the same mass were presented to five board-certified breast radiologists using the graphical user interface described in [7]. Each radiologist was asked to use only the B-mode image and accompanying clinical screenshot to perform two consecutive tasks: (1) classify the content of the mass (i.e., solid, fluid, mixed, or uncertain) and (2) provide a clinical diagnosis (i.e., BI-RADS 2, 3, 4 or 5) [8]. Following classification with only B-mode, the radiologists were presented with the R-SLSC image and asked to perform the same two tasks. Readers had full control over tunable image parameters.

C. Quantitative Metrics

The reader responses were recorded and compared to the ground truth established based on core-needle biopsy. Each

978-1-7281-5448-0/20/$31.00 ©2020 IEEE

mass was further analyzed to investigate potential coherence-based metrics to assist in differentiating solid and fluid-filled masses by measuring lag-one coherence (LOC) [9] and coherence length (CL). Both metrics were obtained by starting with the following equation for a single coherence function:

$$\hat{R}[m] = \frac{1}{N-m} \sum_{i=1}^{N-m} \frac{\sum_{n=n_1}^{n_2} s_i[n] s_{i+m}[n]}{\sqrt{\sum_{n=n_1}^{n_2} s_i^2[n] \sum_{n=n_1}^{n_2} s_{i+m}^2[n]}} \quad (1)$$

where N is the number of elements in the transducer, m is the number of elements between two points in the aperture, or lag, $s_i[n]$ is a time-delayed, zero-mean signal received at element i from depth n. To calculate LOC, Eq. 1 was evaluated at $m = 1$. CL was measured as the first zero-crossing of the coherence function, $\hat{R}[m]$. The mean LOC and CL were each measured from delayed signals within a region of interest (ROI) taken from the center of each breast mass, resulting in the LOC and CL measurements referenced and presented in the following sections.

To compare reader responses and evaluate the ability of CL and LOC to distinguish solid from fluid-filled masses, the sensitivity and specificity of correctly diagnosing cysts were measured as follows:

$$\text{Sensitivity} = \frac{TP}{TP + FN} \quad (2)$$

$$\text{Specificity} = \frac{TN}{TN + FP} \quad (3)$$

where a true positive (TP) was defined as a cyst that was not recommended for biopsy (i.e., BI-RADS 2 or 3), a false negative (FN) was defined as a cyst that was recommended for biopsy (i.e., BI-RADS 4 or 5), a true negative (TN) was defined as a solid mass that was recommended for biopsy (i.e., BI-RADS 4 or 5), and a false positive (FP) was defined a solid mass that was not recommended for biopsy in Task 2 (i.e., BI-RADS 2 or 3). In addition, LOC and CL were parameterized and a threshold was set in order to measure sensitivity and specificity of fluid-filled mass detection. With these measurements, a receiver operating characteristic (ROC) curve was used to compare both metrics and an optimal threshold was determined by measuring the distance to the ideal operating point of (0,1). The masses with a ground truth classified as mixed were omitted from this analysis, considering that they contain a mixture of TP and TN.

III. Results

Fig. 1(a) shows the results of the task-based reader study for simple and complicated cysts (i.e., fluid-filled masses). For simple cysts, shown in the first column, the uncertainty was reduced from 60% with B-mode alone (first row) to 7% with the R-SLSC images included (second row). For

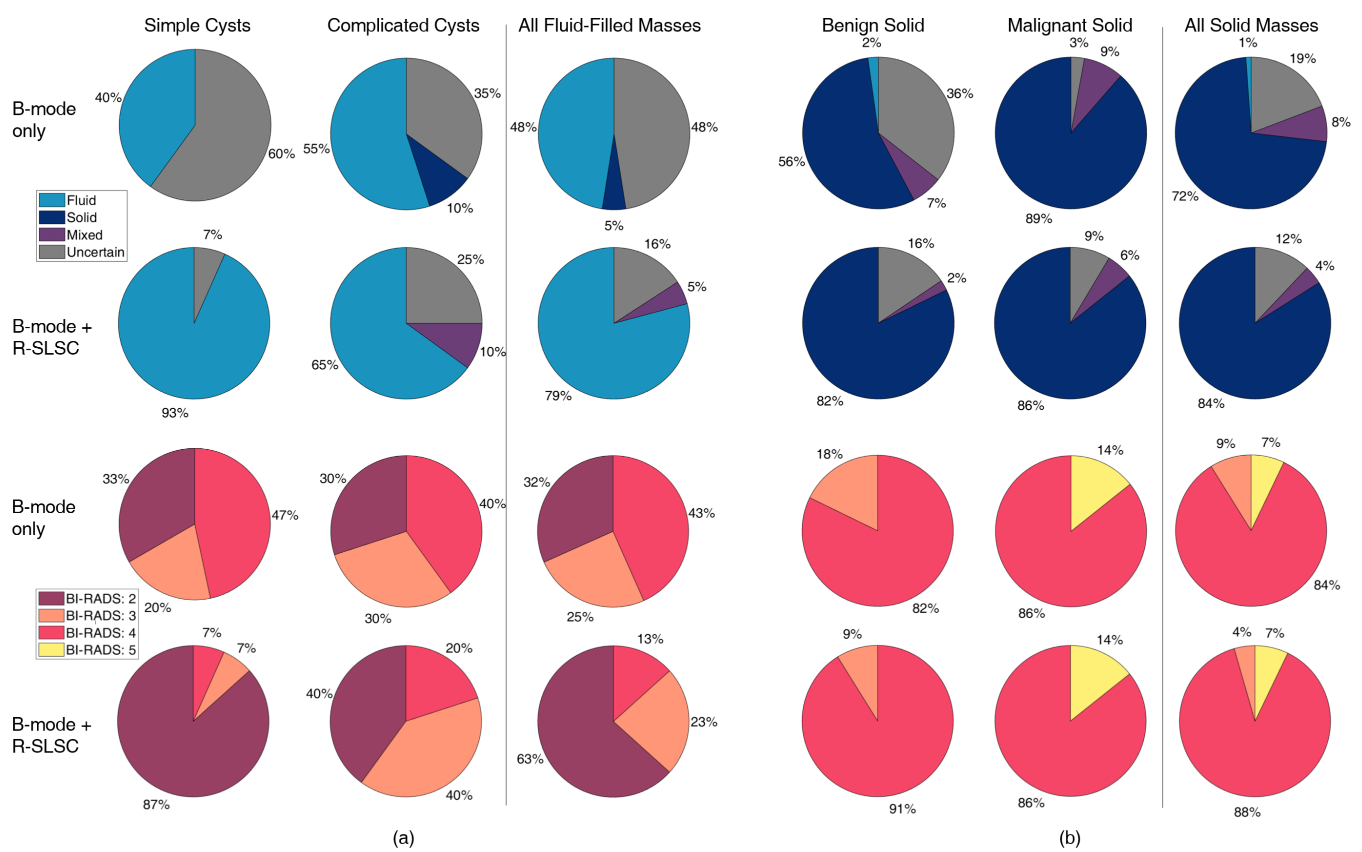

Fig. 1. Pie charts summarizing the results of the task-based reader study for (a) fluid-filled masses and (b) solid masses.

the complicated cysts, shown in the second column, the uncertainty was reduced from 35% with B-mode alone (first row) to 25% with R-SLSC included (second row). In addition, with B-mode alone there were 10% misclassification as solid which were removed with R-SLSC included. Overall, with the inclusion of coherence-based images in decision making, the uncertainty of all fluid-filled mass contents (third columnn of Fig. 1(a)) was reduced from 48% with B-mode only (first row) to 16% (second row) [7]. In addition, the number of simple and complicated cysts recommended for biopsy (indicated by BI-RADS 4 in the presented retrospective BI-RADS classification study) was 47% and 40%, respectively (third row of Fig. 1(a)). With the inclusion of R-SLSC in decision making, these percentages of fluid-filled masses recommended for biopsy were reduced to 7% and 20% for simple and complicated cysts, respectively (fourth row). Overall, the number of fluid-filled masses recommended for biopsy was reduced from 43% with B-mode only (third row) to 13% (fourth row) [7]. Based on these results, the mean $\pm$ standard deviation of the sensitivity and specificity for detecting fluid masses across all readers were 86$\pm$14% and 95$\pm$5%, respectively, as reported in Table I. Additional results describing the readers' performance on all mass types, as well as results broken down by reader are available in [7].

Fig. 1(b) shows the results of the task-based reader study for the benign and malignant solid masses. With B-mode only there is 2% misclassification as fluid for the benign solid masses (first row) that is removed when R-SLSC is included (second row). In addition, the uncertainty is reduced for benign solid masses from 36% with B-mode alone (first row) to 16% with R-SLSC included (second row). The uncertainty for malignant solid masses is increased from 3% with B-mode alone (first row) to 9% with the inclusion of R-SLSC (second row) due to one reader being an outlier. However, the overall uncertainty of all solid mass contents was reduced from 19% (first row) to 12% (second row) with the inclusion of coherence-based images. The BI-RADS classification of solid masses remained similar when comparing retrospective decisions based on B-mode alone (third row) to decisions made with the inclusion of R-SLSC (fourth row). This result is expected because R-SLSC was introduced to distinguish fluid-filled from solid masses and not benign from malignant. Therefore, B-mode alone seems sufficient to recommend biopsy or follow-up for solid masses. Additional results describing the readers' performance on all mass types, as well as results broken down by reader are available in [7].

Fig. 2(a) shows the ROC curve for LOC and CL with the $\times$ and $\circ$ symbols representing the individual reader performance when using B-mode only and B-mode+R-SLSC, respectively. Fig. 2(b) shows the AUC for LOC and CL, which were 0.995 and 0.951, respectively. The optimal threshold value for distinguishing fluid-filled and solid breast masses when using LOC was 0.3. Therefore, LOC $\leq$ 0.3 indicated a fluid-filled mass, while LOC>0.3 indicated a solid mass. The optimal threshold value for distinguishing fluid-filled and solid breast masses when using CL was 6. Therefore, CL$\leq$6 indicated a

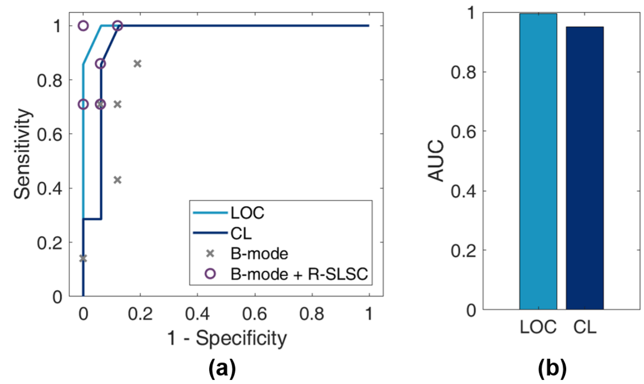

Fig. 2. (a) Receiver operating characteristic (ROC) curve for detection of fluid-filled masses with the individual readers performance for comparison and (b) the associated area under the ROC curve (AUC) for lag-one coherence (LOC) and coherence length (CL).

fluid-filled mass, while CL>6 indicated a solid mass. Based on these optimal thresholds for LOC and CL, LOC provided the best quantitative separation between fluid-filled and solid breast masses with 100% sensitivity and 94% specificity. Using CL=6 as the discriminator resulted in 100% sensitivity and 87% specificity.

Table I summarizes the sensitivity and specificity of: (1) each individual reader, (2) the combination of all readers, and (3) the quantitative coherence-based metrics (i.e., LOC and CL). The reader task consisted of diagnostic decisions using B-mode individually followed by using both B-mode and R-SLSC, while the quantitative metrics did not require any reader input. Overall, LOC and CL improved sensitivity in the majority of cases, with the exception of two readers who had equivalent sensitivity when using both B-mode and R-SLSC imaging. LOC improved or maintained specificity for 4 readers using B-mode only and 3 readers using both B-mode and SLSC. Therefore reader input remains useful to identify true negatives (i.e., solid masses to recommend for biopsy), while LOC can potentially be used as an automated discriminator of true positives (i.e., fluid masses that do not need to be biopsied).

TABLE I
SUMMARY OF SENSITIVITY AND SPECIFICITY FOR DETECTION OF FLUID-FILLED MASSES BASED ON READERS RESPONSES AND OPTIMAL OPERATING POINT OF LOC AND CL.

		Sensitivity (%)	**Specificity (%)**
B-mode	Reader		
	1	14	100
	2	71	88
	3	43	88
	4	86	81
	5	71	94
	All	57 $\pm$ 29	90 $\pm$ 7
B-mode + R-SLSC	Reader		
	1	71	100
	2	100	88
	3	86	94
	4	100	100
	5	71	94
	All	86 $\pm$ 14	95 $\pm$ 5
LOC=0.3		100	94
CL=6		100	87

IV. Discussion

The work presented in this paper investigates the clinical impact of coherence-based beamforming using a retrospective task-based reader study and a quantitative analysis based on two coherence-based metrics. Results demonstrate the added benefit of coherence-based images and metrics, particularly in distinguishing solid from fluid-filled breast masses. In particular, the uncertainty of diagnosing both solid and fluid-filled masses was reduced with the addition of R-SLSC when compared to B-mode alone (see Fig. 1). The increased confidence offered by these coherence-based techniques when a mass is fluid-filled can potentially lead to confident dismissal as a benign mass, rather than a mass requiring follow up or biopsy, helping to reduce patient anxiety and save healthcare system resources.

In addition to its qualitative diagnostic impact, coherence-based metrics such as LOC and CL demonstrated success in quantitatively distinguishing solid from fluid breast masses. These trends can be explained using observations from coherence-based breast ultrasound imaging results [6], [10]. We expect clutter to be removed and spatial coherence to be minimal in fluid-filled masses, and otherwise expect solid masses to appear coherent, resulting in increased coherence within solid masses. LOC and CL are two different metrics to assess the same coherence functions used to make coherence-based images, and are therefore consistent with qualitative observations from and expectations of coherence-based images.

Previous work using contrast differences to distinguish solid and fluid-filled masses demonstrated distinct separability between these two classes [7]. However, measuring contrast in both B-mode and coherence-based images requires the selection of both inside and outside ROIs, which introduces dependence on the outside tissue texture. Conversely, LOC and CL only require one ROI selection within the mass, which is more robust and less prone to selection errors than requiring two distinct ROIs. Therefore, LOC and CL are considered advantageous over the previously reported contrast difference metric [7]. While a threshold of LOC=0.3 was optimal for this study, larger sample sizes are likely required to determine the optimal threshold across a wide variety of breast masses. Despite the small sample size, these results, in tandem with previous reports [6], [7], [10], demonstrate the value of multiple variations of using coherence-based ultrasound information to assist with distinguishing fluid-filled from solid breast masses. The recently introduced CohereNet architecture [11], [12] may also be used for additional automation and reduction of the computational complexity associated with producing spatial correlation information, adding one more item to the list of beneficial applications of coherence-based beamforming previously summarized in [13].

V. Conclusion

This paper summarizes the qualitative and quantitative impact of using coherence information to distinguish fluid from solid breast masses. When using qualitative information from coherence-based images paired with standard B-mode images, the mean sensitivity for detection of fluid-filled masses was 86%, compared to 57% with B-mode alone. In addition, when including LOC as a quantitative coherence-based metric, the sensitivity for detection of fluid-filled masses was improved to 100%. These results are promising for the inclusion of both qualitative and quantitative coherence-based information, requiring both readers and the potential use of automation, in the diagnostic pipeline to reduce the number of unnecessary biopsies and ultimately improve diagnostic certainty in the breast clinic.

VI. Acknowledgements

This research was supported by a Ralph E. Powe Junior Faculty Enhancement Award from Oak Ridge Associated Universities (awarded to M.A.L.B.). The authors thank breast radiologists Emily Ambinder, M.D. and Philip Di Carlo, M.D. for participating in our reader study.

References

[1] M. A. Lediju, M. J. Pihl, J. J. Dahl, and G. E. Trahey, "Quantitative assessment of the magnitude, impact and spatial extent of ultrasonic clutter," *Ultrasonic Imaging*, vol. 30, no. 3, pp. 151–168, 2008.

[2] J.-F. Synnevag, A. Austeng, and S. Holm, "Benefits of minimum-variance beamforming in medical ultrasound imaging," *IEEE Transactions on Ultrasonics, Ferroelectrics, and Frequency Control*, vol. 56, no. 9, pp. 1868–1879, 2009.

[3] M. R. Morgan, G. E. Trahey, and W. F. Walker, "Multi-covariate imaging of sub-resolution targets," *IEEE Transactions on Medical Imaging*, vol. 38, no. 7, pp. 1690–1700, 2019.

[4] M. A. Lediju, G. E. Trahey, B. C. Byram, and J. J. Dahl, "Short-lag spatial coherence of backscattered echoes: Imaging characteristics," *IEEE Transactions on Ultrasonics, Ferroelectrics, and Frequency Control*, vol. 58, no. 7, pp. 1377–1388, 2011.

[5] A. A. Nair, T. D. Tran, and M. A. L. Bell, "Robust short-lag spatial coherence imaging," *IEEE Transactions on Ultrasonics, Ferroelectrics, and Frequency Control*, 2017.

[6] A. Wiacek, O. M. H. Rindal, E. Falomo, K. Myers, K. Fabrega-Foster, S. Harvey, and M. A. L. Bell, "Robust short-lag spatial coherence imaging of breast ultrasound data: Initial clinical results," *IEEE Transactions on Ultrasonics, Ferroelectrics, and Frequency Control*, vol. 66, no. 3, pp. 527–540, 2018.

[7] A. Wiacek, E. Oluyemi, K. Myers, L. Mullen, and M. A. L. Bell, "Coherence-based beamforming increases the diagnostic certainty of distinguishing fluid from solid masses in breast ultrasound exams," *Ultrasound in Medicine & Biology*, vol. 46, no. 6, pp. 1380–1394, 2020.

[8] E. B. Mendelson, W. A. Berg, and C. R. Merritt, "Toward a standardized breast ultrasound lexicon, bi-rads: ultrasound," in *Seminars in Roentgenology*, vol. 36, no. 3. Elsevier, 2001, pp. 217–225.

[9] W. Long, N. Bottenus, and G. E. Trahey, "Lag-one coherence as a metric for ultrasonic image quality," *IEEE Transactions on Ultrasonics, Ferroelectrics, and Frequency Control*, vol. 65, no. 10, pp. 1768–1780, 2018.

[10] A. Wiacek, E. Falomo, K. Myers, O. M. H. Rindal, K. Fabrega-Foster, S. Harvey, and M. A. L. Bell, "Clinical feasibility of coherence-based beamforming to distinguish solid from fluid hypoechoic breast masses," in *2018 IEEE International Ultrasonics Symposium (IUS)*. IEEE, 2018, pp. 1–4.

[11] A. Wiacek, E. Gonzalez, N. Dehak, and M. A. L. Bell, "Coherenet: A deep learning approach to coherence-based beamforming," in *2019 IEEE International Ultrasonics Symposium (IUS)*. IEEE, 2019, pp. 287–290.

[12] A. Wiacek, E. González, and M. A. L. Bell, "Coherenet: A deep learning architecture for ultrasound spatial correlation estimation and coherence-based beamforming," *IEEE Transactions on Ultrasonics, Ferroelectrics, and Frequency Control*, 2020.

[13] J. J. Dahl, D. Hyun, Y. Li, M. Jakovljevic, M. A. L. Bell, W. J. Long, N. Bottenus, V. Kakkad, and G. E. Trahey, "Coherence beamforming and its applications to the difficult-to-image patient," in *2017 IEEE International Ultrasonics Symposium (IUS)*. IEEE, 2017, pp. 1–10.